

**Electronic Supplementary Information**

**for**

Phosphorescent mechanism for single-dopant white  
OLED of FPt: electronic structure and electron  
exchange-induced energy transfer

*Juan Han, Lin Shen, Xuebo Chen\*, Weihai Fang\**

## Section 1, Computational details

### 1.1 Selection of active space

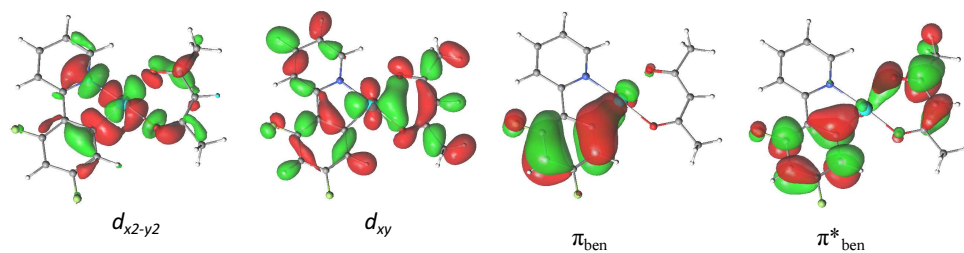
To perform multiconfigurational calculations using CASSCF methods, a set of active orbitals must be selected, and the success of the methods depends on the choice of this set (V. Veryazov, P. Malmqvist, B O. Roos *Int. J. Quantum. Chem.* 2011, **111**, 3329–3338). The numerous test calculations were carried out before optimizations were performed in this work. The compromising must be made between accuracy and computational cost. As shown in Figure SI-1 in the section of supporting information, the  $d_{x^2-y^2}$  orbital of Pt(II) center is used to form Pt-C  $\sigma$  bond. The electron transition originating from  $d_{x^2-y^2}$  orbital inevitably leads to chemical reaction of Pt-C bond fission, which is not closely related to central issue of the photophysical emission in this work. Therefore,  $d_{x^2-y^2}$  orbital is excluded from active space. Unlike  $d_{yz}$ ,  $d_{xz}$ , and  $d_z^2$  orbitals, the symmetry of  $d_{xy}$  orbital does not match with neighboring ligands of pyridinyl or benzene ring from viewpoints of the orientation of electronic transition (see Figure SI-1). The test calculation with  $d_{xy}$  orbital included in the active space shows that occupation number of  $d_{xy}$  orbital was found to be close to 2.0, which indicates  $d_{xy}$  orbital unlikely makes significant contributions to electron transition. We also calculated the vertical excitation with active space containing  $d_{xy}$  orbital. However, no electronic transition associated with  $d_{xy}$  orbital was found by using 5~16 roots stated average calculations. This indicates that  $d_{xy}$  orbital has little possibility to be involved in FC excitation of FPt. Therefore, only  $d_{yz}$ ,  $d_{xz}$ , and  $d_z^2$  orbitals for Pt(II) center were included in active space while the other two orbitals of  $d_{x^2-y^2}$  and  $d_{xy}$  were excluded from active space for saved computational cost.

As shown in Table SI-1 of SI, one  $\pi^*$  orbital of pyridinyl ring with 4 nodes has the lowest orbital energy (1.9 eV at MP4 level of theory) in all virtual orbital and is LUMO orbital. This orbital frequently serve as electron acceptor for metal→ligand ( $M\rightarrow L$ ) and intra-ligand ( $L\rightarrow L'$ ) transitions in most cases of test calculations. As a priority choice, this orbital together with its paired orbital with two nodes localized on the moiety of pyridinyl ring should be included in active space (see Figure SI-2 of SI). One should keep in mind that  $\pi$  orbitals have to appear in active space together with their paired anti-bonding  $\pi^*$  orbital. To further account for the roles of important pyridinyl ligand for electron transition, one more paired  $\pi$ (2 nodes) and  $\pi^*$ (4 nodes) orbital of pyridinyl ring was added to the active space. Similarly, one paired  $\pi$ (2

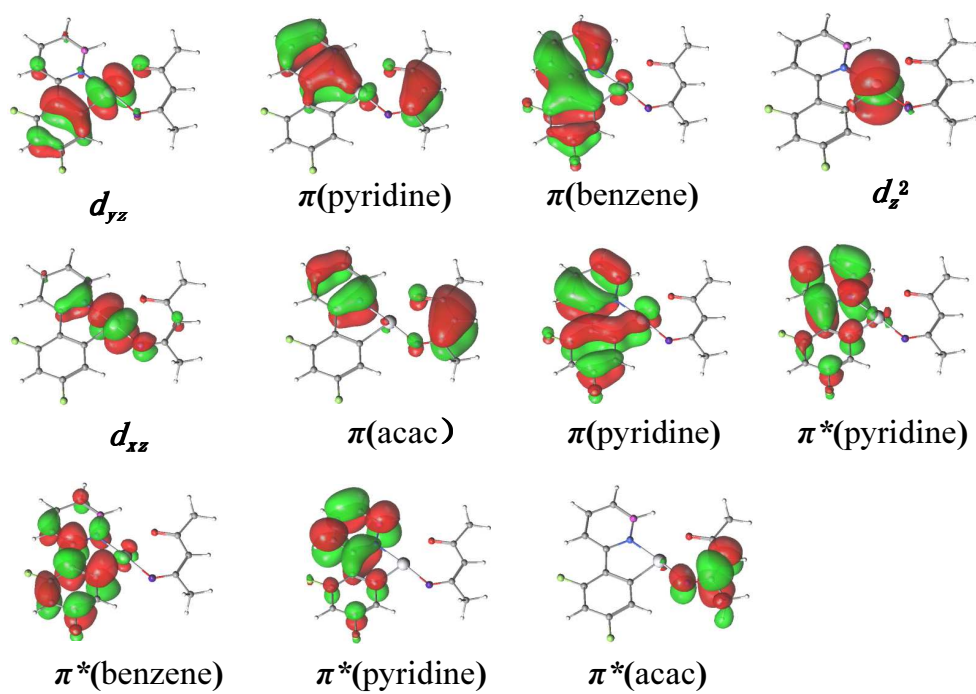
nodes) and  $\pi^*$  (4 nodes) orbital of benzene ring moiety was chosen in active space to describe the ligand localized excitation on benzene ring. Meanwhile, HOMO and LUMO for acac ligand were also included resulting in total 14e/11o active space. The test calculations of vertical excitation were also carried out by using larger active space 16e/13o. The added orbitals originate from one more paired  $\pi$  (2 nodes) and  $\pi^*$  (4 nodes) orbital of benzene ring. The CPU time of test calculations using 16e/13o active space is 3~4 times longer than that at 14e/11o level of theory. As shown in Table SI-2 of SI, the calculated vertical excitation energies for different transitions at CAS(16,13)/6-31g\*/CASPT2 level are blue shifted in comparison with those of experimental observation. This indicates that the use of large active space where more orbitals are included from the ligand of benzene ring does not obviously improve the accuracy but has computational cost significantly increased. As illustrated in Table SI-3 of SI, the various excited states in FC transitions are well differentiated and clearly assigned at CASPT2 calculations by using the CASSCF(14,11) reference wavefunction. No obvious intruder state effect was observed in present calculations. Overall, the present CAS(14e/11o) active space is enough to describe photophysical behavior of FPt, which provides reliable basis for the understanding on the complicated phosphorescent mechanism for single-dopant white OLED.

The analytic frequency calculation is only available when the active space is not larger than 10e/8o in the present stage. Therefore, the active space must be reduced by excluding some orbitals. The  $d_{yz}$  orbital of Pt(II) center and a paired  $\pi$ ,  $\pi^*$  of acac ligand were excluded from the active space in the present second derivatives computations. These frequencies at the CAS(10,8) level of theory were only used to calculate the rate of Dexter energy transfer while the relaxation and radiative paths were computed at CAS(14e,11o)/CASPT2 level of theory.

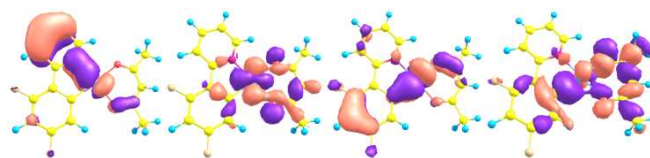
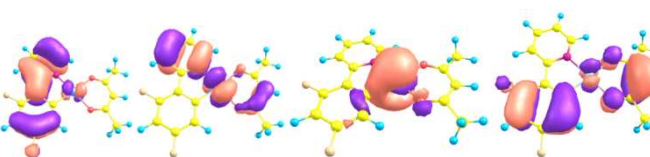
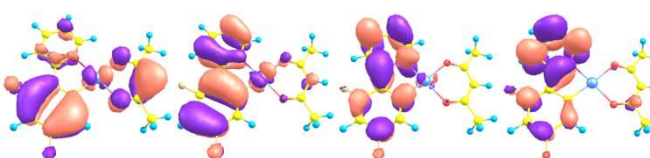
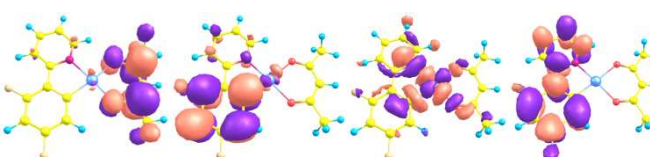
**Figure SI-1** The frontier molecular orbitals of FPT excluded from active space.



**Figure SI-2** The schematic orbitals of FPT used in defining the active space for the CASSCF(14e/11o)//CASPT2 calculation.



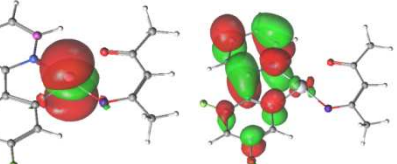
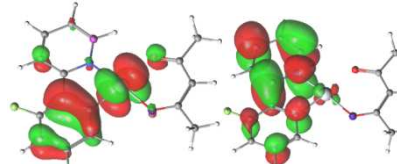
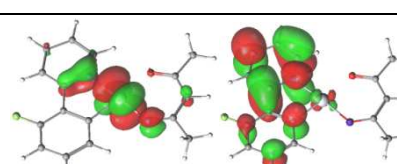
**Table SI-1** The orbital energies are shown for frontier molecular orbitals obtained at MP4 level of theory.

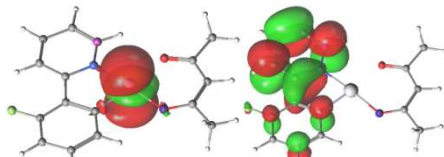
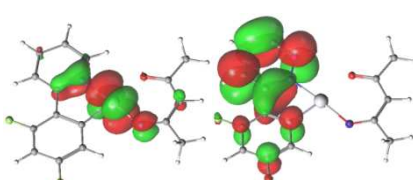
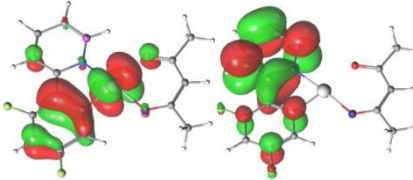
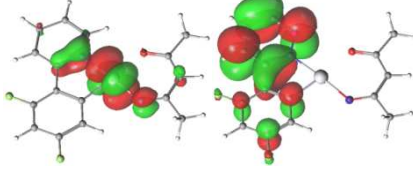
Molecular orbital		E(eV)	Molecular orbital		E(eV)
75	$\pi_{\text{py}}$	-12.0	83	$\pi_{\text{ben}}$	-8.6
76	$d_{\text{xy}}$	-11.4	84	$\pi_{\text{ben}}$	-8.2
77	$d_{\text{yz}}$	-11.3	85	$\pi^*_{\text{py}}$	1.9
78	$\sigma_{\text{dx}2-\text{y}2}$	-11.0	87	$\pi^*_{\text{py}}$	3.0
79	$\pi_{\text{py}}$	-9.2	88	$\pi^*_{\text{acac}}$	3.2
80	$d_{\text{xz}}$	-10.3	91	$\pi^*_{\text{ben}}$	4.3
81	$d_{\text{z}2}$	-9.7	92	$\sigma^*_{\text{dx}2-\text{y}2}$	5.1
82	$\pi_{\text{acac}}$	-8.9	93	$\pi^*_{\text{ben}}$	5.3
The of Molecular orbitals					
					
75	76	77	78		
					
79	80	81	82		
					
83	84	85	87		
					
88	91	92	93		

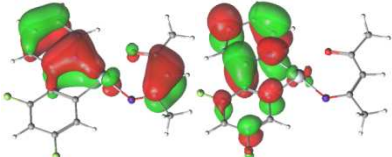
**Table SI-2** The vertical ( $E_{\perp}$ , eV) excitation energies of FPt monomer obtained at CAS(14,11)/6-31g\*/CASPT2 and CAS(16,13)/6-31g\*/CASPT2 level of theory, respectively, and comparison with experimental values.

cas(14,11)	Vertical			exp. $\lambda_{\text{abs}}$	cas(16,13)	Vertical		
	f	$E_{\perp}$	$\lambda_{\text{abs}}(\text{nm})$			f	$E_{\perp}$	$\lambda_{\text{abs}}$
S <sub>0</sub>	-	0	-		S <sub>0</sub>	-	-	-
S <sub>0</sub> →S <sub>MLCTy</sub>	5.74E-02	3.51	353	359	S <sub>0</sub> →S <sub>MLCTy</sub>	1.06E-02	3.89	319
S <sub>0</sub> →S <sub>MLCTx</sub>	5.58E-02	3.92	316	321	S <sub>0</sub> →S <sub>MLCTx</sub>	5.83E-02	4.17	297
S <sub>0</sub> →S <sub>MLCTz<sup>2</sup></sub>	1.23E-02	4.13	300	308	S <sub>0</sub> →S <sub>MLCTz<sup>2</sup></sub>	1.07E-02	4.17	297
S <sub>0</sub> →S <sub>LC</sub>	1.65E-01	4.22	294	273	S <sub>0</sub> →S <sub>MLCTx(II)</sub>	1.50E-02	4.82	257
S <sub>0</sub> →S <sub>MLCTy(II)</sub>	6.60E-03	4.62	268	-	S <sub>0</sub> →S <sub>MLCTy(II)</sub>	7.86E-03	4.84	256
S <sub>0</sub> →S <sub>MLCTx(II)</sub>	1.68E-01	4.89	254	252	S <sub>0</sub> →S <sub>MLCTz<sup>2</sup>(II)</sub>	4.54E-05	5.15	240
S <sub>0</sub> →S <sub>MLCTz<sup>2</sup>(II)</sub>	6.31E-04	5.07	245	-	S <sub>0</sub> →S <sub>MLCTz<sup>2</sup>(III)</sub>	7.33E-03	6.08	203

**Table SI-3** The assignments of different transitions for Franck-Condon geometry of FPT at CAS(14, 11)/6-31G\*/CASPT2 level of theory.

	Configuration with the largest Coefficient			CASSCF reference weight
<b>Root1</b> <b>S0</b>	Occupation	Coefficient	Weight	<b>0.49784</b>
	22222220000	0.90935	0.82692	
<b>Root2</b>  <b>S<sub>MLCT<sub>z2</sub></sub></b>	Occupation	Coefficient	Weight	<b>0.49914</b>
	222u222d000	0.95267	0.90758	
	The character of singly occupied orbitals			
<b>Root3</b>  <b>S<sub>MLCT<sub>yz</sub></sub></b>				<b>0.49266</b>
	Occupation	Coefficient	Weight	
	u222222d000	-0.73363	0.53822	
<b>Root4</b>  <b>S<sub>MLCT<sub>xz</sub></sub></b>	The character of singly occupied orbitals			<b>0.48391</b>
				
	Occupation	Coefficient	Weight	
	2222u22d000	-0.68634	0.47107	
	The character of singly occupied orbitals			
				

	Occupation	Coefficient	Weight		
Root5  $S_{MLCTz^2(II)}$	222u22200d0	0.93812	0.88008	0.49706	
	The character of singly occupied orbitals				
					
Root6  $S_{MLCTxz(II)}$	Occupation	Coefficient	Weight	0.48919	
	2222u22d000	-0.754	0.569		
	The character of singly occupied orbital				
Root7  $S_{MLCTyz(II)}$				0.48792	
	Occupation	Coefficient	Weight		
	u22222200d0	-0.79029	0.62456		
Root7  $S_{MLCTyz(II)}$	The character of singly occupied orbitals			0.48792	
					
	Occupation	Coefficient	Weight		
Root7  $S_{MLCTyz(II)}$	2222u2200d0	-0.42744	0.18271	0.48792	
	The character of singly occupied orbitals				
					

	Occupation	Coefficient	Weight	
	2u22222d00 0	0.80557	0.64895	
<b>Root8</b>				
<b>S<sub>LC</sub></b>				
The character of singly occupied orbitals				
				
<b>0.47108</b>				

**Table SI-4** Frequencies( $\text{cm}^{-1}$ ) are shown for  $S_0$ ,  $T_{\text{LC}}$  and  $T_{\text{MLCTx}}$  minima of FPT monomer at the CAS(10,8)/6-31G\* level of theory.

**$S_0$**

39.1203	44.971	58.8264	73.5431	84.5367
100.3804	105.8128	134.7512	168.9668	173.3876
187.5743	208.3353	222.4109	231.2458	245.7213
264.1892	270.2263	286.8521	296.5515	336.3463
377.7613	385.4392	434.1263	460.8471	469.3151
485.7472	566.6043	568.6996	619.5021	623.5576
633.8177	651.7056	670.1413	700.5833	721.1738
738.1791	749.3251	787.8521	794.5137	835.1159
847.2819	863.6631	896.0832	924.1482	943.9957
988.8421	1019.604	1037.503	1050.425	1084.058
1088.9134	1133.208	1133.533	1134.184	1149.378
1161.247	1162.613	1173.479	1192.687	1209.714
1242.312	1288.916	1303.292	1320.688	1352.476
1400.1389	1402.468	1438.006	1459.492	1518.866
1551.7842	1555.846	1570.64	1577.952	1612.66
1621.1788	1622.078	1626.036	1632.812	1652.73
1702.584	1730.92	1779.652	1784.398	1790.094
1811.5707	3216.059	3217.803	3277.365	3280.512
3308.5309	3310.12	3379.795	3400.885	3401.889
3405.3598	3421.381	3439.192	3466.359	

**T<sub>MLCTx</sub>**

38.3297	41.8998	52.6257	59.0087	79
80.5154	123.5088	131.7901	163.0554	171.6667
187.7882	193.9731	205.1407	215.7128	243.9643
264.3898	268.9828	288.5372	299.686	324.2426
346.2948	391.8664	396.1365	435.6321	457.0523
473.6477	495.3723	567.5552	610.8071	612.895
630.8392	645.4679	646.5065	667.2865	675.5196
682.4214	710.6654	733.6119	747.0198	763.917
781.3153	853.4838	869.3294	923.9336	947.5513
950.2178	972.0121	1008.902	1011.405	1015.95
1033.5246	1056.424	1097.861	1101.261	1135.526
1138.5852	1146.018	1163.894	1172.163	1174.699
1226.6278	1247.291	1295.992	1333.756	1343.487
1381.7724	1404.178	1423.911	1445.937	1496.426
1515.5122	1552.132	1556.249	1557.806	1581.017
1603.9554	1611.425	1618.963	1619.816	1622.106
1634.1517	1675.451	1736.915	1796.218	1810.763
1825.52	3218.091	3221.319	3281.071	3286.193
3310.8923	3317.056	3378.426	3395.773	3407.232
3414.8056	3421.05	3434.562	3436.683	

**T<sub>LC</sub>**

32.1034	38.2573	47.5643	56.3028	74.6265
84.1676	98.8427	129.3698	156.0919	170.7737
183.7328	210.4896	216.8707	219.6214	232.8524
259.269	270.1797	271.3398	286.2073	295.1057
332.1656	375.3719	398.9278	413.4671	427.0339
462.0473	468.9304	496.3371	567.684	598.5243
604.2435	626.3395	632.9585	645.0619	664.1619
688.7567	692.8215	728.7143	737.9445	748.3376
797.926	815.0069	849.5547	908.6962	918.4092
952.9287	965.2483	996.606	1021.666	1038.835
1040.3433	1083.362	1113.31	1123.812	1135.729
1150.0094	1163.06	1173.34	1173.48	1205.373
1249.3893	1255.973	1307.591	1340.393	1356.999
1364.609	1404.901	1424.981	1507.481	1527.336
1531.5313	1551.856	1555.617	1556.347	1566.903
1583.7183	1621.018	1622.129	1626.276	1633.48
1710.1914	1717.764	1764.66	1772.229	1814.01
1877.8922	3216.001	3218.873	3277.094	3281.727
3309.9841	3311.287	3392.812	3401.22	3410.084
3417.6175	3422.169	3427.479	3462.114	

## 1.2 Computational details for energy transfer calculation

The Franck-Condon factor is calculated in the use of eq. 2, 4, 5, and 6 by the following procedure:

(1) The Huang-Rhys factor  $S_j$  and the temperature-related factor  $n_j$  are calculated by using eq. 5 and 6, where  $\omega_j$  is the vibrational frequency of the harmonic oscillator on the corresponding electronic state for the  $j$ th normal mode, which can be obtained from the frequency analysis by using Gaussian 03 program. The  $\Delta Q$  is the displacement of the oscillator during the transition between two electronic states, which is calculated as

$$\Delta Q = |L| \cdot \Delta q$$

where  $\Delta q$  is the displacement of the mass-weighted Cartesian coordinates, and  $|L|$  is the normal mode matrix obtained from the frequency analysis.

(2) The correlation function  $G_j(t)$  can be calculated easily by applying eq. 5 and 6 into eq. 4.

(3) Finally, the Franck-Condon factor ( $FC$ ) is obtained by applying  $G_j(t)$  into eq. 2. The saddle-point method yields

$$FC = \sqrt{\frac{1}{2\pi\hbar^2 a}} \exp\left\{\sum_j S_j [(n_j + 1)e^{it^*\omega_j} + n_j e^{-it^*\omega_j} - (2n_j + 1)] + it^*\omega_{i \rightarrow f}\right\}$$

where

$$a = \sum_j S_j \omega_j^2 [(n_j + 1)e^{it^*\omega_j} + n_j e^{-it^*\omega_j}]$$

and  $t^*$  is the saddle-point value determined by

$$\sum_j S_j \omega_j [(n_j + 1)e^{it^*\omega_j} - n_j e^{-it^*\omega_j}] + \omega_{i \rightarrow f} = 0$$

On the other hand, the Hamiltonian matrix element is calculated by using eq. 8, where the two-electron integrals ( $ij|kl$ ) and the singly occupied orbital coefficients  $c$  can be obtained from the CASSCF calculation on the FPT dimer in the triplet charge-transfer state by using Gaussian 03 program.

### 1.3 Estimation on the average distance between two molecules

The molecular volume ( $V$ ) of FPt can be directly calculated according to  $V = 100M / (\rho \times \text{wt} \times N_A)$ , where  $M = 484$  g/mol is the molecular weight of FPt,  $\rho = 1.2$  g/cm<sup>3</sup> is typical density of organic films, and  $N_A$  is the Avogadro's number.<sup>1</sup> Then the average distance between two molecules ( $R$ ) is obtained by  $V = 4\pi R^3/3$ .

[1] J. Kalinowski, M. Cocchi, V. Fattori, L. Murphy, J. A. G. Williams, *Organic electronics*, 2010, **11**, 724-730.

### 1.4 Error analysis

As mentioned in the Computational Methods, the Franck-Condon factor and Hamiltonian matrix element were computed independently during the calculation of energy transfer rate. Thus, there are two main error sources of the Dexter energy transfer calculation. One comes from the Franck-Condon factor calculation. In the present work, two approximations, the harmonic and displaced approximation were introduced. The two approximations with their errors have been discussed for several decades, and the results agree well with the experimental findings when the structural rigidity of molecule during its excitation and relaxation processes is strong. The electronic structure calculation shows that the FPt monomer is consistent with this case, so the error from the Franck-Condon factor calculation is small. Another comes from the Hamiltonian matrix element calculation. It should be noted that no more approximation was introduced in Eq. 8, and all parameters in the equation were obtained from the wavefunction of FPt dimer in the triplet charge-transfer state. Thus, the error from the Hamiltonian matrix element calculation is mainly determined by

the accuracy of electronic structure calculations. Although the CASSCF calculation on FPt dimer with 70 atoms and 2 heavy Pt atoms is very difficult, the calculated properties such as geometry and dipole moment show that it does not lead to obvious errors compared with the CASSCF calculation on the FPt monomer.

## Section 2, Results and Discussion

**2.1 The nature of excited states and absorption spectrum of FPt.** Table 1 summarized the vertical and adiabatic transition energies for the FPt monomer as well as other properties. To assess the accuracy of the electronic structure calculations, we first analyze the optical absorption characteristics. The FPt in the ground state adopts  $C_s$  symmetry that is confirmed to be a minimum by frequency calculations. The geometric structures of FPt in all excited states were calculated to have planar or quasi-planar arrangement. For the convenience of discussion and comparison, the orientations N-Pt-O1 and C-Pt-O2 are defined to be  $x$  and  $y$  axis of molecular plane (see Figure 1 for the Cartesian axes), respectively. As shown in Table 1,  $S_0 \rightarrow S_{MLCT_y}$  transition was found to originate from the promotion of one electron from the  $d_{yz}$  orbital of Pt to a  $\pi^*$  orbital mainly localized in the pyridinyl ring moiety. Mulliken population analysis shows that ~0.5 electron transfers from the Pt to the pyridinyl ring upon  $S_0 \rightarrow S_{MLCT_y}$  excitation along  $x$  direction. The dipole moment consequently increases from -4.67 D in the ground state to 0.48 D in the  $S_{MLCT_y}$  state along  $x$  direction. Meanwhile, the electron redistribution also results in a dipole moment change (3.52 D) along  $y$  direction. This is different from the cases in Pt-4 with high  $C_{2v}$  symmetry where the change of dipole moment occurs along the specific one direction of  $y$  axis.<sup>1</sup> In the  $y$  direction of Pt-4, the electron donor Cl atom pushes the electron to the Pt(II) center, whereas the electron withdrawing F substitutes attract the electron towards the benzene ring.<sup>1</sup> In the  $x$  direction of Pt-4, however, the two symmetric pyridinyl rings on the both sides of  $C_2$  axis exert the same influence on Pt(II) center. Although there are large changes of dipole moment along  $x$  and  $y$  direction, respectively, upon  $S_0 \rightarrow S_{MLCT_y}$  excitation of FPt, the coupling of dipole moment along two dimensions results in the smaller total dipole moment change (0.82 D) in comparison with that of Pt-4 (3.54 D). This is caused by decreasing symmetry from  $C_{2v}$  of Pt-4 to  $C_s$  of FPt. Consequently, the direction-specific charge transfer of FPt induced by electron excitation does not proceed as well as that in Pt-4.

As illustrated in Table 1, one singly occupied electron for  $S_0 \rightarrow S_{MLCT_y}$  transition of FPt mainly distributes on the pyridinyl moiety. In contrast with this, the corresponding transition for Pt-4 leads to singly occupied electron being populated in the benzene ring. To address this discrepancy, we analyzed the orbital energies of Pt-4 and FPt at MP4 level. The energy of  $\pi^*$  orbital mainly located on pyridinyl moiety is 2.40 eV lower than that located on benzene ring in FPt, while in Pt-4 the energy of  $\pi^*$

orbital on pyridinyl ring is 0.08 eV slightly higher than that on benzene ring. This indicates that  $\pi^*$  orbital of benzene ring functions as an efficient acceptor when electron in Pt(II)  $d_{yz}$  orbital is excited in Pt-4. However, it becomes energetically unfavorable for  $S_0 \rightarrow S_{MLCT_y}$  transition in FPt and the  $\pi^*$  orbital on pyridinyl ring alternatively severs as major acceptor of excited electron.

The inter-ligand charge-transfer (ILCT) state was found in Pt-4 originating from electron transfer along the direction from pyridinyl to benzene ring.<sup>1</sup> However,  $S_0 \rightarrow S_{ILCT}$  or  $S_0 \rightarrow T_{ILCT}$  transition was not found in vertical excitations of FPt (see Table 1) and minima optimization attempts for ILCT of FPt lead to failure. To account for these differences between FPt and Pt-4, we calculated the orbital energies of different ligands for these two molecules at MP4 level of theory to explore changes of transition possibility varying with chemical environment. Quantitatively, the energy level of  $\pi^*$  orbital on benzene moiety is close to that on pyridine ring ( $\Delta E = 0.08$  eV) in Pt-4. Therefore, occurrence of electron migration between two moieties is feasible. In contrast, large energy gap (2.40 eV) between the  $\pi^*$  orbitals on benzene moiety and pyridinyl moiety of FPt leads to high energy level of ILCT state beyond low energy excitation at  $\lambda > 300$  nm. We also examined an FPt analogue without F substitution, Pt(II) [2-pyridinato-*N*, $C^{2'}$ ](2,4-pentanedionato) ( $C^N\text{Pt}(O^O)$ ). The  $\pi^*$  orbital on pyridinyl is found to be  $\sim 2.67$  eV lower than the  $\pi^*$  orbital on benzene ring. Therefore, benzene ring moiety without F substitution leads to large  $\pi^*$  orbital energy gap which reduces the migration possibilities of excited  $d_{yz}$  electron towards the direction of C-Pt-O2 (*y* axis). This allows electron transfer to exhibit much more character of the unique or specific direction (N-Pt-O1(*x* axis)) in comparison with the case in FPt. This can partially account for why the quantum efficiency of blue emission of FPt ( $\Phi=0.02$ ) is lower than that of its analogue without F substitution ( $\Phi=0.15$ ).<sup>2</sup>

Like  $S_0 \rightarrow S_{MLCT_y}$  transition of FPt, both  $S_0 \rightarrow S_{MLCT_x}$  and  $S_0 \rightarrow S_{MLCT_z}^2$  are MLCT excitations. They are attributed to the electron transition from  $d_{xz}$  and  $d_z^2$  to the  $\pi^*$  orbital of pyridine ring, respectively. Mulliken population analysis shows that  $\sim 0.5$  electron is transferred from Pt to pyridinyl ring along the *x* direction for the  $S_0 \rightarrow S_{MLCT_z}^2$  transitions. The dipole moments for  $S_0 \rightarrow S_{MLCT_x}$  and  $S_0 \rightarrow S_{MLCT_z}^2$  are consequently increased to 0.17 and 1.77 D along the *x* direction and 7.34 and 7.30 D along the *y* direction, respectively. As shown in Table 1,  $S_0 \rightarrow S_{LC}$  and  $S_0 \rightarrow T_{LC}$  transitions mainly take place on phenylpyridinyl ligand and are assigned to be ligand

centered (LC) excitation. The wave function of unpaired electron in  $S_0 \rightarrow T_{LC}$  transition can be presented as

$$\phi_{T_{LC}^1} = 11.4\%d_{yz} + 58.9\%\pi_{pyridine} + 29.7\%\pi_{benzene}$$

and

$$\phi_{T_{LC}^2} = 2.9\%d_{xz} + 66.2\%\pi_{pyridine} + 30.9\%\pi_{benzene}$$

This unequivocally reveals that  $S_0 \rightarrow T_{LC}$  is ligand center transition with small contribution from Pt. In contrast with  $S_0 \rightarrow T_{LC}$  excitation,  $S_0 \rightarrow S_{LC}$  transition is partially intruded by  $d_{yz}$  orbital of Pt(II) center, where wave functions of singly occupied electrons are expressed as

$$\phi_{S_{LC}^1} = 23.2\%d_{yz} + 55.5\%\pi_{pyridine} + 21.3\%\pi_{benzene}$$

and

$$\phi_{S_{LC}^2} = 2.1\%d_{xz} + 1.7\%p_z(\text{Pt}) + 84.3\%\pi_{pyridine} + 11.9\%\pi_{benzene}$$

As illustrated in Table 1,  $S_0 \rightarrow S_{mix}$  and  $S_0 \rightarrow S_{LC}$  transitions have the largest oscillator strength ( $f = \sim 0.160$ ) whose vertical excitation energies are calculated to be 4.89 eV (254 nm) and 4.22 eV (294 nm), respectively. It is very difficult to determine the nature of  $S_{mix}$  excitation that probably originates from the mixture among several MLCT and LC transitions. In consistent with our computation, two intense absorption bands of FPt were observed to peak at 252 and 273 nm in solution.<sup>2-5</sup> Thompson and co-workers assigned these two bands to ligand-centered transition. Meanwhile, they considered MLCT transition to be the weak absorption at  $\lambda > 300$  nm region. Three absorption bands are experimentally observed at 308, 321, and 359 nm,<sup>2-5</sup> which are very close to our theoretical values, i.e., 301 nm (4.12 eV), 316 nm (3.92 eV) and 353 nm (3.51 eV). The nature of three absorption bands is assigned to  $S_0 \rightarrow S_{MLCTz}^2$ ,  $S_0 \rightarrow S_{MLCTx}$  and  $S_0 \rightarrow S_{MLCTy}$  excitation, respectively, in this work. The weak  $S_0 \rightarrow T_n$  vertical excitations were also calculated by using the spin-orbit coupling computation (see Table 1). The lowest lying  $S_0 \rightarrow T_{LC}$  absorption was calculated at 446 nm (2.78 eV,  $f = 2.44 \times 10^{-6}$ ) that agrees well with experimental value 469 nm.<sup>3-5</sup> Overall, the present electronic structure calculations on the monomer of FPt give accurate electronic transition energies and provide clear molecular orbital pictures for the MLCT and LC transitions.

- [1] J. Han, X. B. Chen, L. Shen, Y. Chen, W. H. Fang and H. B. Wang, *Chem. Eur. J.*, 2011, **17**, 13971.
- [2] J. Brooks, Y. Babayan, S. Lamansky, P. I. Djurovich, I. Tsyba, R. Bau and M. E. Thompson, *Inorg. Chem.*, 2002, **41**, 3055.
- [3] X. H. Yang, Z. X. Wang, S. Madakuni, J. Li and G. E. Jabbour, *Adv. Mater.*, 2008, **20**, 2405.
- [4] A. F. Rausch, H. H. H. Homeier and H. Yersin, *Top. Organomet. Chem.*, 2010, **29**, 193.
- [5] B. W. Ma, P. I. Djurovich and M. E. Thompson, *Coordin. Chem. Rev.*, 2005, **249**, 1501.

**Figures SI-3** The optimized structures and the character of singly occupied orbitals of  $T_{CT}(\text{dimer})$  state.

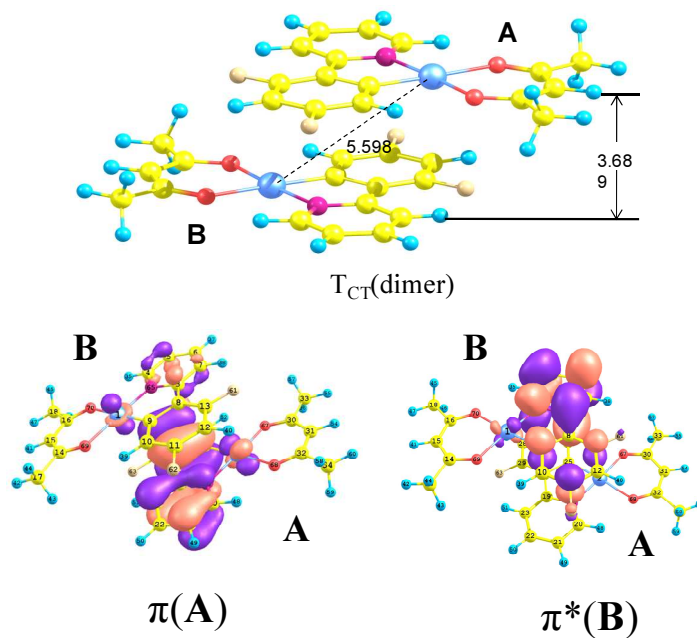


**Table SI-5** The absolute energies (A. E.) in Hartree the optimized structures of FPt at the CAS(14,11)/6-31G\*/CASPT2 level of theory.

States	A. E. (CASSCF)	A. E. (CASPT2)
S <sub>0</sub>	-1134.83706	-1137.82793
S <sub>MLCT<sub>y</sub></sub>	-1134.73295	-1137.71599
S <sub>0</sub> *(S <sub>MLCT<sub>y</sub></sub> )	-1134.83974	-1137.82583
S <sub>MLCT<sub>z</sub>2</sub>	-1134.73439	-1137.69460
S <sub>0</sub> *(S <sub>MLCT<sub>z</sub>2</sub> )	-1134.83911	-1137.82661
S <sub>LC</sub>	-1134.63395	-1137.67945
S <sub>0</sub> *(S <sub>LC</sub> )	-1134.83599	-1137.82395
SCT(S <sub>MLCT<sub>y</sub></sub> )	-1134.73068	-1137.71331
SCT(T <sub>MLCT<sub>x</sub></sub> )	-1134.72864	-1137.71915
T <sub>LC</sub>	-1134.73447	-1137.74186
S <sub>0</sub> *(T <sub>LC</sub> )	-1134.81992	-1137.81400
T <sub>MLCT<sub>x</sub>(T<sub>MLCT<sub>y</sub></sub>)</sub>	-1134.74975	-1137.73468
S <sub>0</sub> *	-1134.83178	-1137.82011
T <sub>MLCT<sub>y</sub></sub>	-1134.67763	-1137.70507
S <sub>0</sub> *(T <sub>MLCT<sub>y</sub></sub> )	-1134.83718	-1137.82621
T <sub>MLCT<sub>z</sub>2</sub>	-1134.73863	-1137.70166
S <sub>0</sub> *(T <sub>MLCT<sub>z</sub>2</sub> )	-1134.83733	-1137.82615
SCT(T <sub>MLCT<sub>x</sub></sub> ) <sup>a</sup>	-1134.73933	-1137.72788
SCT(T <sub>LC</sub> ) <sup>a</sup>	-1134.72313	-1137.71351

<sup>a</sup> SCT(T<sub>MLCT<sub>x</sub></sub>) and SCT(T<sub>LC</sub>) are avoided crossings.

**Table SI-6** The absolute energies (A. E.) in Hartree and relative energies (R. E.) in eV for the point of radiative relaxation path of the FPt monomer induced by the excitation obtained by CASSCF(14e/11o)/CASPT2 computations.

	A. E.	R. E.
<b>Path 1</b>		
FC-S <sub>MLCTy</sub>	-1137.699110	3.51
S <sub>MLCTy-1</sub>	-1137.714893	3.08
S <sub>MLCTy-2-min</sub>	-1137.715840	3.05
S <sub>MLCTy-3</sub>	-1137.715325	3.06
S <sub>MLCTy-4</sub>	-1137.714938	3.07
SCT(S <sub>MLCTy</sub> )	-1137.713308	3.12
<b>Path 2</b>		
SCT(T <sub>MLCTX</sub> )	-1137.719172	2.96
SCT→T <sub>MLCTX-1</sub>	-1137.716940	3.02
SCT→T <sub>MLCTX-2</sub>	-1137.717699	3.00
SCT→T <sub>MLCTX-3</sub>	-1137.732380	2.60
SCT→T <sub>MLCTX-4</sub>	-1137.734489	2.54
T <sub>MLCTX-min</sub>	-1137.734489	2.54
<b>Path 3</b>		
FC-T <sub>LC</sub>	-1137.713412	3.12
T <sub>LC-1</sub>	-1137.731123	2.63
T <sub>LC-2</sub>	-1137.733381	2.57
T <sub>LC-3</sub>	-1137.734489	2.54
T <sub>LC-4</sub>	-1137.734494	2.54
T <sub>LC-min</sub>	-1137.741860	2.34

**Section 3,** Cartesian coordinate of the optimized structures for FPt at the CAS(14,11)/6-31G\* level of theory

S<sub>0</sub>

PT	0.008892	0.606872	0.000218
C1	-1.583646	-1.829693	0.000081
C2	-2.946428	0.068026	0.000087
C3	-4.098699	-0.692971	-0.000022
C4	-3.969554	-2.080330	-0.000077
C5	-2.721328	-2.647918	-0.000024
C6	-0.174926	-2.275564	0.000083
C7	0.801890	-1.232686	0.000148
C8	2.133941	-1.562005	0.000096
C9	2.511130	-2.904724	-0.000022
C10	1.611692	-3.929560	-0.000087
C11	0.260917	-3.583910	-0.000024
C12	1.979114	2.830011	-0.000016
C13	1.003604	3.828897	-0.000230
C14	-0.387797	3.613451	-0.000009
C15	3.433835	3.231781	0.000006
C16	-1.308066	4.810503	-0.000005
H1	-2.961487	1.138638	0.000122
H2	-5.059113	-0.214714	-0.000071
H3	-4.842614	-2.706943	-0.000171
H4	-2.607849	-3.710151	-0.000083
H5	2.893418	-0.804502	0.000123
H6	1.916946	-4.956951	-0.000191

H7	1.341977	4.845433	-0.000402
H8	3.573492	4.304357	-0.000201
H9	3.915056	2.807207	0.874416
H10	3.915182	2.806849	-0.874159
H11	-1.947578	4.760164	-0.874844
H12	-1.947273	4.760394	0.875070
H13	-0.776164	5.752054	-0.000220
F1	-0.610851	-4.597497	-0.000122
F2	3.806817	-3.195579	-0.000093
N	-1.730070	-0.492783	0.000139
O1	1.797117	1.584605	0.000246
O2	-0.961764	2.506431	0.000240
S <sub>MLCTy</sub>			
PT	0.582582	0.075646	-0.003397
C1	-1.968395	1.408444	0.002985
C2	-0.142970	2.971668	-0.001512
C3	-0.970620	4.023839	0.008093
C4	-2.400030	3.793976	0.017376
C5	-2.865226	2.499879	0.014791
C6	-2.260661	0.007954	0.001846
C7	-1.149289	-0.870473	0.001073
C8	-1.304804	-2.269341	0.002134
C9	-2.563832	-2.772789	0.003696
C10	-3.704916	-1.951749	0.004091
C11	-3.539910	-0.608988	0.002632
C12	2.954289	-1.742367	0.013472

C13	3.870457	-0.700166	0.020194
C14	3.561821	0.677712	0.007013
C15	3.457159	-3.163398	0.024556
C16	4.683515	1.682933	0.006948
H1	0.922010	3.092314	-0.010220
H2	-0.570182	5.019991	0.007027
H3	-3.085487	4.620521	0.026431
H4	-3.917894	2.305982	0.021503
H5	-0.456273	-2.924544	0.002025
H6	-4.687882	-2.381999	0.005553
H7	4.908383	-0.963283	0.033073
H8	4.536534	-3.226297	0.040338
H9	3.054581	-3.671333	0.894208
H10	3.080090	-3.675730	-0.853925
H11	4.595424	2.299364	-0.881069
H12	4.566593	2.332978	0.866963
H13	5.661380	1.223141	0.031185
F1	-4.628857	0.155211	0.005255
F2	-2.761080	-4.089518	0.006018
N	-0.584021	1.671082	-0.003643
O1	1.685997	-1.652577	-0.002342
O2	2.414144	1.172353	-0.007911
$S_{MLCT_z^2}$			
PT	0.012566	0.578771	-0.077649
C1	-1.655086	-1.776023	-0.022454
C2	-2.931609	0.249736	-0.079889

C3	-4.091017	-0.414365	-0.004475
C4	-4.070256	-1.857975	0.087213
C5	-2.854061	-2.501110	0.087088
C6	-0.296382	-2.234149	-0.031163
C7	0.714011	-1.274046	-0.044839
C8	2.068330	-1.614348	-0.041586
C9	2.398171	-2.937897	-0.027755
C10	1.434653	-3.947014	-0.017410
C11	0.127306	-3.581236	-0.020206
C12	2.109822	2.693585	0.013947
C13	1.211385	3.740790	0.042802
C14	-0.194521	3.625042	-0.025360
C15	3.588787	2.979548	0.061628
C16	-1.027414	4.885448	-0.018435
H1	-2.888835	1.316909	-0.135175
H2	-5.022024	0.120910	-0.005900
H3	-4.983958	-2.412668	0.167305
H4	-2.812766	-3.567623	0.163983
H5	2.837573	-0.869103	-0.054346
H6	1.717319	-4.980970	-0.011468
H7	1.618749	4.728335	0.101163
H8	3.812336	4.035136	0.117483
H9	4.013456	2.474087	0.921714
H10	4.051389	2.558723	-0.824016
H11	-1.621879	4.921283	-0.924494
H12	-1.712847	4.852576	0.821117

H13	-0.424856	5.780504	0.048110
F1	-0.790280	-4.546028	-0.010370
F2	3.678739	-3.305114	-0.029481
N	-1.718650	-0.381885	-0.080725
O1	1.851753	1.456333	-0.052087
O2	-0.834499	2.559500	-0.094268
S <sub>LC</sub>			
PT	0.005378	0.615708	0.000000
C1	-1.614310	-1.821940	0.000000
C2	-2.950476	0.107539	0.000000
C3	-4.108708	-0.620871	0.000000
C4	-4.061750	-2.038652	0.000000
C5	-2.768737	-2.626118	0.000000
C6	-0.254252	-2.263164	0.000000
C7	0.746453	-1.212571	0.000000
C8	2.113151	-1.559093	0.000000
C9	2.462940	-2.878760	0.000000
C10	1.511334	-3.935008	0.000000
C11	0.203010	-3.619135	0.000000
C12	2.058193	2.782806	0.000000
C13	1.110349	3.804237	0.000000
C14	-0.288762	3.625319	0.000000
C15	3.523201	3.149356	0.000000
C16	-1.181283	4.842654	0.000000
H1	-2.983839	1.177583	0.000000
H2	-5.045635	-0.100058	0.000000

H3	-4.944787	-2.636980	0.000000
H4	-2.670373	-3.689380	0.000000
H5	2.865144	-0.793806	0.000000
H6	1.835504	-4.959711	0.000000
H7	1.474094	4.812150	0.000000
H8	3.689039	4.218389	0.000000
H9	3.995280	2.714936	0.874680
H10	3.995280	2.714936	-0.874680
H11	-1.822159	4.804752	-0.874362
H12	-1.822159	4.804752	0.874362
H13	-0.629043	5.772173	0.000000
F1	-0.681705	-4.607118	0.000000
F2	3.737473	-3.235042	0.000000
N	-1.718226	-0.420991	0.000000
O1	1.841433	1.540752	0.000000
O2	-0.890185	2.534426	0.000000

SCT( $S_{MLCT_y}/T_{MLCT_x}$ )

PT	0.001570	0.584272	0.000000
C1	-1.663283	-1.757025	0.000000
C2	-2.938483	0.250974	0.000000
C3	-4.100514	-0.417658	0.000000
C4	-4.078660	-1.853712	0.000000
C5	-2.855050	-2.494273	0.000000
C6	-0.304648	-2.243111	0.000000
C7	0.707821	-1.267230	0.000000
C8	2.061767	-1.622587	0.000000

C9	2.393336	-2.942533	0.000000
C10	1.430023	-3.952386	0.000000
C11	0.120230	-3.591950	0.000000
C12	2.128080	2.701283	0.000000
C13	1.219552	3.762955	0.000000
C14	-0.172375	3.631278	0.000000
C15	3.609846	2.985583	0.000000
C16	-1.034516	4.866382	0.000000
H1	-2.919021	1.319456	0.000000
H2	-5.023859	0.121366	0.000000
H3	-4.988409	-2.415606	0.000000
H4	-2.805932	-3.560851	0.000000
H5	2.839183	-0.884533	0.000000
H6	1.711518	-4.987391	0.000000
H7	1.622819	4.755786	0.000000
H8	3.826062	4.045061	0.000000
H9	4.062632	2.530833	0.874607
H10	4.062632	2.530833	-0.874607
H11	-1.676831	4.847212	-0.874238
H12	-1.676831	4.847212	0.874238
H13	-0.457349	5.780888	0.000000
F1	-0.785856	-4.569289	0.000000
F2	3.675419	-3.306232	0.000000
N	-1.717123	-0.357568	0.000000
O1	1.840966	1.472954	0.000000
O2	-0.799312	2.545271	0.000000

T<sub>LC</sub>

PT	-0.000360	0.630690	-0.002270
C1	-1.545480	-1.876730	0.001280
C2	-2.926580	0.060250	-0.005400
C3	-4.107200	-0.737040	-0.004510
C4	-3.964410	-2.178960	0.000530
C5	-2.745120	-2.717380	0.003420
C6	-0.207410	-2.264920	0.001370
C7	0.793940	-1.202230	-0.002720
C8	2.122680	-1.523230	-0.004690
C9	2.518520	-2.857810	-0.002390
C10	1.602280	-3.913390	0.002330
C11	0.285780	-3.612830	0.004090
C12	1.970630	2.856600	-0.000530
C13	0.997730	3.854050	0.000820
C14	-0.397080	3.640910	0.000900
C15	3.425920	3.257110	0.000330
C16	-1.313970	4.840730	0.003220
H1	-2.983040	1.131090	-0.008620
H2	-5.067570	-0.262690	-0.007530
H3	-4.841740	-2.797870	0.001690
H4	-2.614510	-3.778090	0.006840
H5	2.872690	-0.755850	-0.007680
H6	1.934150	-4.933470	0.004440
H7	1.335940	4.870690	0.002480
H8	3.567100	4.329640	0.001850

H9	3.906890	2.830950	0.874150
H10	3.907280	2.833340	-0.874430
H11	-1.953910	4.793750	-0.871490
H12	-1.953040	4.791000	0.878430
H13	-0.779280	5.780570	0.004460
F1	-0.589530	-4.623320	0.008510
F2	3.811460	-3.158710	-0.004150
N	-1.731420	-0.453250	-0.002540
O1	1.789520	1.608730	-0.001750
O2	-0.970750	2.536690	-0.000420
T <sub>MLCTx</sub>			
PT	0.576070	0.075901	-0.008177
C1	-1.951725	1.431952	0.010294
C2	-0.054285	2.949541	-0.004968
C3	-0.854461	4.012207	0.017472
C4	-2.299269	3.829807	0.043617
C5	-2.803953	2.536543	0.037499
C6	-2.278600	0.024991	0.004679
C7	-1.187383	-0.856421	-0.001109
C8	-1.366145	-2.244823	-0.004105
C9	-2.638299	-2.731109	-0.000698
C10	-3.761609	-1.899852	0.004064
C11	-3.563917	-0.556356	0.006295
C12	2.916888	-1.782560	0.037755
C13	3.869474	-0.787583	0.042914
C14	3.603363	0.609587	0.009551

C15	3.343662	-3.227429	0.068804
C16	4.759460	1.577497	0.005836
H1	1.012886	3.034685	-0.027349
H2	-0.429934	4.998431	0.012461
H3	-2.956234	4.677355	0.066342
H4	-3.861489	2.373046	0.052442
H5	-0.530863	-2.916398	-0.008841
H6	-4.752538	-2.310049	0.005837
H7	4.897472	-1.087170	0.070228
H8	4.418415	-3.345987	0.096917
H9	2.907349	-3.705516	0.939202
H10	2.950683	-3.730351	-0.808250
H11	4.700942	2.183794	-0.891403
H12	4.658182	2.242606	0.856121
H13	5.721334	1.085669	0.045127
F1	-4.637232	0.232612	0.013865
F2	-2.846537	-4.046097	-0.005029
N	-0.535388	1.641723	-0.003244
O1	1.642008	-1.631735	0.005717
O2	2.476024	1.121756	-0.022661
T <sub>MLCTy</sub>			
PT	0.000163	0.578722	0.000000
C1	-1.623098	-1.791405	0.000000
C2	-2.952580	0.185825	0.000000
C3	-4.098861	-0.523243	0.000000
C4	-4.024505	-1.953726	0.000000

C5	-2.814981	-2.561074	0.000000
C6	-0.277526	-2.236594	0.000000
C7	0.729138	-1.233003	0.000000
C8	2.106496	-1.557015	0.000000
C9	2.473511	-2.856191	0.000000
C10	1.517824	-3.896951	0.000000
C11	0.190303	-3.578115	0.000000
C12	2.062782	2.750475	0.000000
C13	1.113526	3.777115	0.000000
C14	-0.271054	3.603114	0.000000
C15	3.526916	3.104788	0.000000
C16	-1.166237	4.814439	0.000000
H1	-2.948016	1.257484	0.000000
H2	-5.043684	-0.014407	0.000000
H3	-4.924534	-2.540235	0.000000
H4	-2.743653	-3.628171	0.000000
H5	2.848404	-0.783135	0.000000
H6	1.826593	-4.924327	0.000000
H7	1.482378	4.782404	0.000000
H8	3.698976	4.171957	0.000000
H9	3.992119	2.663437	0.874462
H10	3.992119	2.663437	-0.874462
H11	-1.806633	4.773620	-0.874374
H12	-1.806633	4.773620	0.874374
H13	-0.615477	5.744682	0.000000
F1	-0.690188	-4.583373	0.000000

F2	3.761534	-3.209164	0.000000
N	-1.727868	-0.402035	0.000000
O1	1.837438	1.514033	0.000000
O2	-0.881540	2.501955	0.000000
T <sub>MLCTz2</sub>			
PT	0.581248	0.078358	-0.016385
C1	-1.994129	1.407041	0.010941
C2	-0.171678	2.964093	-0.016504
C3	-0.997684	4.017087	0.013684
C4	-2.425306	3.791078	0.046139
C5	-2.887786	2.492545	0.044644
C6	-2.281366	-0.004630	0.012104
C7	-1.173998	-0.868353	0.000767
C8	-1.315649	-2.261729	-0.003355
C9	-2.573558	-2.780320	0.006845
C10	-3.715219	-1.972909	0.019443
C11	-3.551451	-0.625832	0.022117
C12	2.985070	-1.731406	0.043802
C13	3.903910	-0.699067	0.076947
C14	3.595350	0.683051	0.032563
C15	3.471943	-3.157957	0.075188
C16	4.718445	1.688129	0.051201
H1	0.893266	3.081299	-0.042763
H2	-0.595414	5.012398	0.010234
H3	-3.109571	4.616827	0.073639
H4	-3.939521	2.296138	0.070861

H5	-0.462201	-2.910476	-0.014072
H6	-4.696636	-2.405336	0.026313
H7	4.939970	-0.964507	0.126596
H8	4.549605	-3.232136	0.127653
H9	3.034916	-3.660242	0.931319
H10	3.119938	-3.668661	-0.814517
H11	4.657127	2.293902	-0.846138
H12	4.580013	2.348675	0.899914
H13	5.694614	1.227279	0.108246
F1	-4.645751	0.133496	0.034854
F2	-2.750465	-4.100870	0.002362
N	-0.616083	1.664342	-0.020481
O1	1.714465	-1.631012	-0.016867
O2	2.450921	1.166103	-0.024662

SCT( $T_{MLCT\alpha}/T_{LC}$ )	(Avoided crossing)		
PT	0.579352	0.063757	-0.067686
C1	-1.967053	1.460520	-0.065335
C2	-0.124017	2.979732	-0.209583
C3	-0.924021	4.052856	-0.109568
C4	-2.335822	3.851498	0.048280
C5	-2.811592	2.561197	0.125842
C6	-2.272007	0.038556	-0.062389
C7	-1.192755	-0.856331	-0.106617
C8	-1.348726	-2.239974	-0.031623
C9	-2.625226	-2.713309	0.017641

C10	-3.756831	-1.891472	0.048163
C11	-3.555375	-0.550400	0.050314
C12	2.950030	-1.806725	0.000360
C13	3.900888	-0.816812	0.044907
C14	3.630397	0.587262	0.071302
C15	3.363988	-3.254373	-0.009011
C16	4.784103	1.555130	0.136143
H1	0.940865	3.074830	-0.301840
H2	-0.503867	5.041156	-0.140295
H3	-3.004640	4.686254	0.149428
H4	-3.859470	2.386600	0.264610
H5	-0.512688	-2.911328	-0.026686
H6	-4.744833	-2.305665	0.101642
H7	4.931365	-1.107956	0.058663
H8	4.438763	-3.378220	0.013516
H9	2.929042	-3.751783	0.851090
H10	2.966450	-3.731033	-0.898197
H11	4.741406	2.205007	-0.731017
H12	4.662111	2.177346	1.015684
H13	5.745973	1.063590	0.171466
F1	-4.624172	0.240325	0.122760
F2	-2.830487	-4.030314	0.052573
N	-0.590880	1.693104	-0.166671
O1	1.669403	-1.664352	0.005857
O2	2.507546	1.101262	0.026015

Path1

$S_{MLCTy-l}$

PT	0.000305	0.581735	0.000000
C1	-1.653163	-1.782773	0.000000
C2	-2.960257	0.233043	0.000000
C3	-4.112873	-0.450460	0.000000
C4	-4.074536	-1.897344	0.000000
C5	-2.847835	-2.528334	0.000000
C6	-0.295765	-2.253055	0.000000
C7	0.715243	-1.260689	0.000000
C8	2.080405	-1.590126	0.000000
C9	2.423916	-2.904574	0.000000
C10	1.468509	-3.931055	0.000000
C11	0.154346	-3.596435	0.000000
C12	2.109905	2.713532	0.000000
C13	1.191455	3.760081	0.000000
C14	-0.204195	3.617391	0.000000
C15	3.582884	3.022016	0.000000
C16	-1.068264	4.850088	0.000000
H1	-2.944365	1.306078	0.000000
H2	-5.045852	0.081522	0.000000
H3	-4.982614	-2.471044	0.000000
H4	-2.793099	-3.596879	0.000000
H5	2.842204	-0.834790	0.000000
H6	1.766923	-4.961700	0.000000
H7	1.584050	4.756274	0.000000

H8	3.786821	4.083612	0.000000
H9	4.034045	2.565487	0.876510
H10	4.034045	2.565487	-0.876510
H11	-1.708008	4.827139	-0.875510
H12	-1.708008	4.827139	0.875510
H13	-0.492788	5.765286	0.000000
F1	-0.736776	-4.585187	0.000000
F2	3.708103	-3.256873	0.000000
N	-1.730381	-0.375674	0.000000
O1	1.849487	1.477571	0.000000
O2	-0.835212	2.533938	0.000000

$S_{MLCTy-2}$

PT	0.573315	0.046707	0.000000
C1	-1.868983	1.572574	0.000000
C2	0.081224	2.970590	0.000000
C3	-0.655965	4.092401	0.000000
C4	-2.092002	3.982481	0.000000
C5	-2.673883	2.727027	0.000000
C6	-2.282589	0.185007	0.000000
C7	-1.225492	-0.774507	0.000000
C8	-1.469280	-2.132047	0.000000
C9	-2.779374	-2.568748	0.000000
C10	-3.839469	-1.690335	0.000000
C11	-3.576859	-0.336647	0.000000
C12	2.796467	-1.940232	0.000000
C13	3.790998	-0.964757	0.000000

C14	3.578367	0.420492	0.000000
C15	3.192668	-3.393743	0.000000
C16	4.770129	1.342596	0.000000
H1	1.152162	3.004541	0.000000
H2	-0.160286	5.044578	0.000000
H3	-2.709820	4.862225	0.000000
H4	-3.737689	2.628562	0.000000
H5	-0.674092	-2.853655	0.000000
H6	-4.853073	-2.041160	0.000000
H7	4.805649	-1.305036	0.000000
H8	4.264198	-3.533532	0.000000
H9	2.765191	-3.871848	0.874478
H10	2.765191	-3.871848	-0.874478
H11	4.715791	1.981587	-0.874608
H12	4.715791	1.981587	0.874608
H13	5.711433	0.811194	0.000000
F1	-4.636614	0.471744	0.000000
F2	-3.017661	-3.879581	0.000000
N	-0.480951	1.726902	0.000000
O1	1.548561	-1.753740	0.000000
O2	2.465897	1.001501	0.000000
S <sub>MLCTy-3</sub>			
PT	0.578684	0.041751	0.000000
C1	-1.868002	1.563692	0.000000
C2	0.069049	2.982172	0.000000
C3	-0.676335	4.093203	0.000000

C4	-2.121027	3.974977	0.000000
C5	-2.680314	2.714730	0.000000
C6	-2.270992	0.194347	0.000000
C7	-1.224055	-0.772874	0.000000
C8	-1.474553	-2.133880	0.000000
C9	-2.785636	-2.556928	0.000000
C10	-3.843605	-1.663716	0.000000
C11	-3.575431	-0.322660	0.000000
C12	2.812007	-1.951808	0.000000
C13	3.801947	-0.971994	0.000000
C14	3.588255	0.412918	0.000000
C15	3.210874	-3.403880	0.000000
C16	4.777097	1.337285	0.000000
H1	1.139560	3.024812	0.000000
H2	-0.199204	5.055186	0.000000
H3	-2.744750	4.849009	0.000000
H4	-3.745672	2.599001	0.000000
H5	-0.681253	-2.855487	0.000000
H6	-4.860732	-2.006565	0.000000
H7	4.818310	-1.308177	0.000000
H8	4.282649	-3.542713	0.000000
H9	2.783821	-3.882434	0.874444
H10	2.783821	-3.882434	-0.874444
H11	4.719957	1.976365	-0.874313
H12	4.719957	1.976365	0.874313
H13	5.720082	0.808889	0.000000

F1	-4.612881	0.513441	0.000000
F2	-3.051868	-3.862409	0.000000
N	-0.467211	1.717514	0.000000
O1	1.562187	-1.768398	0.000000
O2	2.474204	0.993592	0.000000
S <sub>MLCTy-4</sub>			
PT	0.574462	0.037017	0.000000
C1	-1.867672	1.564491	0.000000
C2	0.076219	2.978905	0.000000
C3	-0.665130	4.092626	0.000000
C4	-2.109991	3.978662	0.000000
C5	-2.672996	2.722974	0.000000
C6	-2.274746	0.191170	0.000000
C7	-1.230657	-0.776263	0.000000
C8	-1.482348	-2.140393	0.000000
C9	-2.789410	-2.562142	0.000000
C10	-3.851349	-1.666976	0.000000
C11	-3.584264	-0.329933	0.000000
C12	2.812830	-1.951271	0.000000
C13	3.800370	-0.968744	0.000000
C14	3.584185	0.415366	0.000000
C15	3.217159	-3.401724	0.000000
C16	4.770694	1.343084	0.000000
H1	1.147644	3.014477	0.000000
H2	-0.187378	5.054156	0.000000
H3	-2.728233	4.856158	0.000000
H4	-3.737737	2.612003	0.000000

H5	-0.686688	-2.859308	0.000000
H6	-4.867038	-2.014219	0.000000
H7	4.817814	-1.302308	0.000000
H8	4.289524	-3.536794	0.000000
H9	2.791944	-3.881836	0.874450
H10	2.791944	-3.881836	-0.874450
H11	4.711593	1.982193	-0.874194
H12	4.711593	1.982193	0.874194
H13	5.715603	0.818121	0.000000
F1	-4.623254	0.503296	0.000000
F2	-3.062682	-3.865561	0.000000
N	-0.464590	1.715248	0.000000
O1	1.562515	-1.772889	0.000000
O2	2.469008	0.992949	0.000000

## Path2

### SCT $\rightarrow$ T<sub>MLCTx-1</sub>

PT	-0.007409	0.585988	0.000000
C1	-1.649763	-1.773276	0.000000
C2	-2.948529	0.218836	0.000000
C3	-4.103213	-0.462437	0.000000
C4	-4.064125	-1.899462	0.000000
C5	-2.833567	-2.526538	0.000000
C6	-0.286645	-2.244098	0.000000
C7	0.717685	-1.258774	0.000000
C8	2.072791	-1.601177	0.000000
C9	2.417248	-2.918927	0.000000

C10	1.463603	-3.936878	0.000000
C11	0.150128	-3.587837	0.000000
C12	2.099858	2.721137	0.000000
C13	1.190798	3.774244	0.000000
C14	-0.203818	3.632960	0.000000
C15	3.576142	3.012352	0.000000
C16	-1.072319	4.862880	0.000000
H1	-2.940515	1.287724	0.000000
H2	-5.032121	0.066657	0.000000
H3	-4.967643	-2.472165	0.000000
H4	-2.770058	-3.593057	0.000000
H5	2.842621	-0.855159	0.000000
H6	1.752617	-4.969810	0.000000
H7	1.588044	4.769335	0.000000
H8	3.791155	4.072145	0.000000
H9	4.026177	2.554628	0.874417
H10	4.026177	2.554628	-0.874417
H11	-1.714314	4.839061	-0.874163
H12	-1.714314	4.839061	0.874163
H13	-0.500817	5.780899	0.000000
F1	-0.749838	-4.571952	0.000000
F2	3.703236	-3.269678	0.000000
N	-1.720690	-0.374647	0.000000
O1	1.821801	1.489135	0.000000
O2	-0.823002	2.544929	0.000000

SCT→T<sub>MLCTx-2</sub>

PT	-0.006231	0.583754	0.000000
C1	-1.663123	-1.757494	0.000000
C2	-2.944247	0.246009	0.000000
C3	-4.104902	-0.425042	0.000000
C4	-4.078505	-1.862356	0.000000
C5	-2.853532	-2.500273	0.000000
C6	-0.304215	-2.240334	0.000000
C7	0.708776	-1.263917	0.000000
C8	2.060806	-1.618272	0.000000
C9	2.393614	-2.939012	0.000000
C10	1.431017	-3.948503	0.000000
C11	0.120675	-3.587877	0.000000
C12	2.119808	2.700212	0.000000
C13	1.220082	3.761305	0.000000
C14	-0.175727	3.632342	0.000000
C15	3.598605	2.978380	0.000000
C16	-1.033334	4.869883	0.000000
H1	-2.926795	1.314784	0.000000
H2	-5.029102	0.112234	0.000000
H3	-4.987045	-2.427058	0.000000
H4	-2.799443	-3.567311	0.000000
H5	2.837193	-0.879081	0.000000
H6	1.710899	-4.983947	0.000000
H7	1.626099	4.752850	0.000000
H8	3.822968	4.036233	0.000000
H9	4.044581	2.516700	0.874417

H10	4.044581	2.516700	-0.874417
H11	-1.675514	4.851733	-0.874163
H12	-1.675514	4.851733	0.874163
H13	-0.453748	5.782819	0.000000
F1	-0.787945	-4.564007	0.000000
F2	3.676454	-3.301105	0.000000
N	-1.715466	-0.354871	0.000000
O1	1.830883	1.470714	0.000000
O2	-0.804494	2.549820	0.000000

SCT $\rightarrow$ T<sub>MLCTx-3</sub>

PT	-0.010614	0.581347	0.000000
C1	-1.663123	-1.757494	0.000000
C2	-2.944247	0.246009	0.000000
C3	-4.104902	-0.425042	0.000000
C4	-4.078505	-1.862356	0.000000
C5	-2.853532	-2.500273	0.000000
C6	-0.304215	-2.240334	0.000000
C7	0.708776	-1.263917	0.000000
C8	2.060806	-1.618272	0.000000
C9	2.393614	-2.939012	0.000000
C10	1.431017	-3.948503	0.000000
C11	0.120675	-3.587877	0.000000
C12	2.115425	2.697805	0.000000
C13	1.215699	3.758898	0.000000
C14	-0.180110	3.629935	0.000000
C15	3.594222	2.975973	0.000000

C16	-1.037717	4.867476	0.000000
H1	-2.926795	1.314784	0.000000
H2	-5.029102	0.112234	0.000000
H3	-4.987045	-2.427058	0.000000
H4	-2.799443	-3.567311	0.000000
H5	2.837193	-0.879081	0.000000
H6	1.710899	-4.983947	0.000000
H7	1.621716	4.750443	0.000000
H8	3.818585	4.033826	0.000000
H9	4.040198	2.514293	0.874417
H10	4.040198	2.514293	-0.874417
H11	-1.679897	4.849326	-0.874163
H12	-1.679897	4.849326	0.874163
H13	-0.458131	5.780412	0.000000
F1	-0.787945	-4.564007	0.000000
F2	3.676454	-3.301105	0.000000
N	-1.711083	-0.352464	0.000000
O1	1.826500	1.468307	0.000000
O2	-0.808877	2.547413	0.000000
SCT $\rightarrow$ T <sub>MLCTx-4</sub>			
PT	-0.023791	0.575388	0.000000
C1	-1.635566	-1.796098	0.000000
C2	-2.943583	0.253770	0.000000
C3	-4.084755	-0.429686	0.000000
C4	-4.056744	-1.886046	0.000000
C5	-2.824301	-2.525583	0.000000

C6	-0.270926	-2.269888	0.000000
C7	0.720509	-1.278341	0.000000
C8	2.081591	-1.603819	0.000000
C9	2.430916	-2.920656	0.000000
C10	1.485513	-3.949187	0.000000
C11	0.170623	-3.609656	0.000000
C12	2.071653	2.710058	0.000000
C13	1.175336	3.761351	0.000000
C14	-0.230747	3.635659	0.000000
C15	3.550392	2.989558	0.000000
C16	-1.074907	4.885194	0.000000
H1	-2.912947	1.324058	0.000000
H2	-5.020431	0.096855	0.000000
H3	-4.969276	-2.449495	0.000000
H4	-2.774682	-3.594675	0.000000
H5	2.838583	-0.845117	0.000000
H6	1.788406	-4.977977	0.000000
H7	1.579823	4.752902	0.000000
H8	3.775031	4.046929	0.000000
H9	3.993581	2.525250	0.875116
H10	3.993581	2.525250	-0.875116
H11	-1.715468	4.871867	-0.874828
H12	-1.715468	4.871867	0.874828
H13	-0.485408	5.791488	0.000000
F1	-0.728304	-4.592551	0.000000
F2	3.716478	-3.266897	0.000000

N	-1.694510	-0.364957	0.000000
O1	1.794417	1.466839	0.000000
O2	-0.863307	2.564672	0.000000

Path3

T<sub>LC-1</sub>

PT	0.634705	0.008013	0.000000
C1	-1.874454	1.563655	0.000000
C2	0.063923	2.925977	0.000000
C3	-0.751655	4.105215	0.000000
C4	-2.207940	3.963454	0.000000
C5	-2.735972	2.744516	0.000000
C6	-2.276517	0.182862	0.000000
C7	-1.210554	-0.786134	0.000000
C8	-1.524137	-2.132256	0.000000
C9	-2.865391	-2.524740	0.000000
C10	-3.899242	-1.632041	0.000000
C11	-3.579831	-0.281228	0.000000
C12	2.861088	-1.958055	0.000000
C13	3.855369	-0.976757	0.000000
C14	3.639077	0.407097	0.000000
C15	3.271620	-3.410155	0.000000
C16	4.835370	1.328913	0.000000
H1	1.134488	2.957721	0.000000
H2	-0.282363	5.068518	0.000000
H3	-2.845037	4.827319	0.000000
H4	-3.796731	2.623439	0.000000

H5	-0.758157	-2.882864	0.000000
H6	-4.922665	-1.950997	0.000000
H7	4.872217	-1.313725	0.000000
H8	4.344743	-3.543329	0.000000
H9	2.848913	-3.892754	0.874404
H10	2.848913	-3.892754	-0.874404
H11	4.784636	1.968260	-0.874943
H12	4.784636	1.968260	0.874943
H13	5.777524	0.798119	0.000000
F1	-4.612266	0.565852	0.000000
F2	-3.144719	-3.821861	0.000000
N	-0.460237	1.733646	0.000000
O1	1.618956	-1.781794	0.000000
O2	2.530592	0.983530	0.000000
T <sub>LC-2</sub>			
PT	0.627327	0.007445	0.000000
C1	-1.884509	1.552201	0.000000
C2	0.060599	2.922045	0.000000
C3	-0.744043	4.120755	0.000000
C4	-2.206553	3.972490	0.000000
C5	-2.732922	2.753929	0.000000
C6	-2.274051	0.180658	0.000000
C7	-1.211535	-0.791200	0.000000
C8	-1.522421	-2.137729	0.000000
C9	-2.861651	-2.533663	0.000000
C10	-3.894755	-1.640525	0.000000

C11	-3.576517	-0.290857	0.000000
C12	2.857283	-1.958508	0.000000
C13	3.850746	-0.976486	0.000000
C14	3.633028	0.406941	0.000000
C15	3.268340	-3.410578	0.000000
C16	4.828712	1.329414	0.000000
H1	1.131434	2.978111	0.000000
H2	-0.269168	5.080785	0.000000
H3	-2.823033	4.850669	0.000000
H4	-3.792256	2.613921	0.000000
H5	-0.754563	-2.886377	0.000000
H6	-4.918036	-1.960420	0.000000
H7	4.867881	-1.312668	0.000000
H8	4.341449	-3.543756	0.000000
H9	2.845634	-3.893280	0.874355
H10	2.845634	-3.893280	-0.874355
H11	4.777779	1.968682	-0.874979
H12	4.777779	1.968682	0.874979
H13	5.771062	0.798943	0.000000
F1	-4.606556	0.558949	0.000000
F2	-3.140622	-3.831061	0.000000
N	-0.451977	1.738011	0.000000
O1	1.615395	-1.782161	0.000000
O2	2.523989	0.982844	0.000000
T <sub>LC-3</sub>			
PT	0.629623	0.008395	0.000000

C1	-1.885661	1.553336	0.000000
C2	0.058894	2.926681	0.000000
C3	-0.749970	4.122736	0.000000
C4	-2.210095	3.970921	0.000000
C5	-2.734727	2.752428	0.000000
C6	-2.272085	0.180819	0.000000
C7	-1.209242	-0.790107	0.000000
C8	-1.520476	-2.136365	0.000000
C9	-2.859925	-2.532144	0.000000
C10	-3.894008	-1.639260	0.000000
C11	-3.575567	-0.290458	0.000000
C12	2.856393	-1.960161	0.000000
C13	3.850693	-0.978525	0.000000
C14	3.634829	0.405401	0.000000
C15	3.267285	-3.412230	0.000000
C16	4.831643	1.326585	0.000000
H1	1.129788	2.990088	0.000000
H2	-0.276927	5.083017	0.000000
H3	-2.829592	4.847298	0.000000
H4	-3.794174	2.609645	0.000000
H5	-0.751841	-2.884217	0.000000
H6	-4.917385	-1.958938	0.000000
H7	4.867538	-1.315629	0.000000
H8	4.340427	-3.545299	0.000000
H9	2.844635	-3.894910	0.874399
H10	2.844635	-3.894910	-0.874399

H11	4.781385	1.965982	-0.874934
H12	4.781385	1.965982	0.874934
H13	5.773511	0.795251	0.000000
F1	-4.604928	0.560641	0.000000
F2	-3.138803	-3.829264	0.000000
N	-0.449684	1.740995	0.000000
O1	1.614590	-1.783666	0.000000
O2	2.526737	0.982804	0.000000
T <sub>LC-4</sub>			
PT	0.629925	0.008371	0.000000
C1	-1.886825	1.553661	0.000000
C2	0.059046	2.927693	0.000000
C3	-0.750127	4.122353	0.000000
C4	-2.208749	3.971118	0.000000
C5	-2.734092	2.752203	0.000000
C6	-2.271529	0.180606	0.000000
C7	-1.208977	-0.789791	0.000000
C8	-1.520130	-2.136503	0.000000
C9	-2.858984	-2.532586	0.000000
C10	-3.893485	-1.639612	0.000000
C11	-3.575365	-0.291106	0.000000
C12	2.855171	-1.960139	0.000000
C13	3.849104	-0.978251	0.000000
C14	3.633756	0.405834	0.000000
C15	3.267007	-3.412018	0.000000
C16	4.831184	1.326232	0.000000

H1	1.129922	2.991810	0.000000
H2	-0.276382	5.082441	0.000000
H3	-2.829361	4.846758	0.000000
H4	-3.793644	2.610913	0.000000
H5	-0.751253	-2.884061	0.000000
H6	-4.916669	-1.959826	0.000000
H7	4.865914	-1.315430	0.000000
H8	4.340206	-3.544472	0.000000
H9	2.844666	-3.894993	0.874390
H10	2.844666	-3.894993	-0.874390
H11	4.781234	1.965641	-0.874940
H12	4.781234	1.965641	0.874940
H13	5.772758	0.794376	0.000000
F1	-4.604649	0.560153	0.000000
F2	-3.137887	-3.829629	0.000000
N	-0.448014	1.741171	0.000000
O1	1.613145	-1.784548	0.000000
O2	2.526084	0.983904	0.000000